THE JOURNAL OF PHYSICAL CHEMISTRY B LETTERS

2006, *110,* 9751−9754
Published on Web 04/29/2006

Versatile Fabrication of Distorted Cubic Mesoporous Silica Film Using CTAB Together with a Hydrophobic Organic Additive

Sajo P. Naik,[†,‡] Toshiyuki Yokoi,[†] Wei Fan,[†] Yukichi Sasaki,[§] Ta-chen Wei,[||] Hugh W. Hillhouse,[||] and Tatsuya Okubo*[,†,‡]

Department of Chemical System Engineering, The University of Tokyo, PRESTO, JST, 7-3-1, Hongo, Bunkyo-ku, Tokyo 113-8656, Japan, Japan Fine Ceramics Center, 2-4-1 Mutsuno, Atsuta-ku, Nagoya, 456-8587, Japan, and School of Chemical Engineering, Purdue University, West Lafayette, Indiana 47907

Received: February 10, 2006; In Final Form: March 29, 2006

We have succeeded in the fabrication of distorted cubic *R*-3*m* mesoporous silica film with 3D open mesostructure providing high pore accessibility from the surface−air interface of the film. The film fabrication involves a unique approach of adding 1,3,5- triisopropylbenzene (TIPB) to the silica/cetyltrimethylammoniumbromide (CTAB) coating sol during its preparation. The addition of TIPB induces the formation of spheroid micelles, promoting *R*-3*m* mesostructure in the film. This phase does not exist in the corresponding binary phase diagram of CTAB surfactant.

Introduction

Thin films of mesoporous silica[1,2] are of scientific and technological importance as they have potential applications in advanced electronics and optics. For their widespread commercial applications, economical processing with mesophase selection and orientation control is considered to be the key element. From the structural consideration for the film, 3D open mesostructures such as *Ia*3*d*, *Pm*3*n*, *Im*3*m*, *R*-3*m*, etc., are promising for various applications including membrane separation and sensing since the direct pore accessibility from the surface−air interface is provided in such structures. In this brief communication, we will provide a unique approach for the fabrication of highly porous distorted cubic *R*-3*m* mesoporous silica film with 3D open mesostructure using cetyltrimethylammoniumbromide (CTAB) as a structure-directing agent together with a hydrophobic organic additive, 1,3,5- triisopropylbenzene (TIPB). This is the first report on the formation of *R*-3*m* silica film using CTAB since the corresponding phase does not exist in the phase diagram of CTAB in water or in other solvents.[3,4] The film has a very high density of open mesopores from the surface−air interface.

Experimental Procedure

The silica precursor solution was first prepared by stirring 2.0 g of tetraethyl orthosilicate (TEOS, Wako) with 0.5 g of HCl (0.1 M, Wako) and 1.0 g of 98% ethanol (Wako) at room temperature for 1 h. The surfactant solution containing 0.52 g of CTAB (Aldrich), 0.45 g of 1,3,5-triisopropylbenzene (TIPB, Across), and 3.5 g of ethanol was prepared by stirring at room temperature (25 °C) for 1 h. The surfactant solution was then slowly mixed with the silica precursor solution for 15 min at room temperature to form the silica−surfactant coating sol. The film was fabricated by dip coating at 5 cm/min under ambient conditions using pre-cleaned thin glass cover slips as substrates. For comparison, *p*6*mm* hexagonal films were prepared from the sol of the same composition but at [TIPB] = 0. The as-coated film was maintained at room temperature for 24 h, followed by calcination at 500 °C for 5 h in air. Grazing-angle of incidence small-angle X-ray scattering (GISAXS) patterns were collected from films at beamline 8-ID-E, Advanced Photon Source (wavelength 0.1631 nm, angle of incidence 0.22 degree), Argonne National Laboratory. The substrate was positioned vertically, and an elongated beam stop was used to block the main incident and reflected beams. The 2D intensity data are plotted as a function of $2\theta_f$ and θ_f, the in-plane and out-of-plane exit angles, respectively, with an arbitrary intensity scale. Diffraction spot patterns were simulated and overlaid on experimental data using NANOCELL.[5] This code uses the distorted wave Born approximation (DWBA) to account for reflection and refraction effects.[6] The transmission electron microscopy (TEM) images of the calcined mesoporous silica film were recorded on JEM 2010 electron microscope (JEOL) at an acceleration voltage of 200 kV. The field emission scanning electron microscopy (FE-SEM) measurements were carried out on S-5200 instrument (Hitachi) at an accelerating voltage of 30 kV, without any surface coating of the film samples. The N_2 adsorption/desorption isotherms of the calcined mesoporous silica films peeled from the substrate were determined at 77 K on Autosorb-1 instrument (Quantachrome Co.).

Results and Discussion

One of the plausible approaches for the fabrication of films with high pore accessibility is to form cubic or cage-like mesostructures that are inherently interconnected through pores

* Corresponding author. Fax: +81-3-5800-3806; Tel: +81-3-5841-7348. E-mail: okubo@chemsys.t.u-tokyo.ac.jp
[†] The University of Tokyo.
[‡] PRESTO.
[§] Japan Fine Ceramics Center.
[||] Purdue University.

10.1021/jp060869p CCC: $33.50

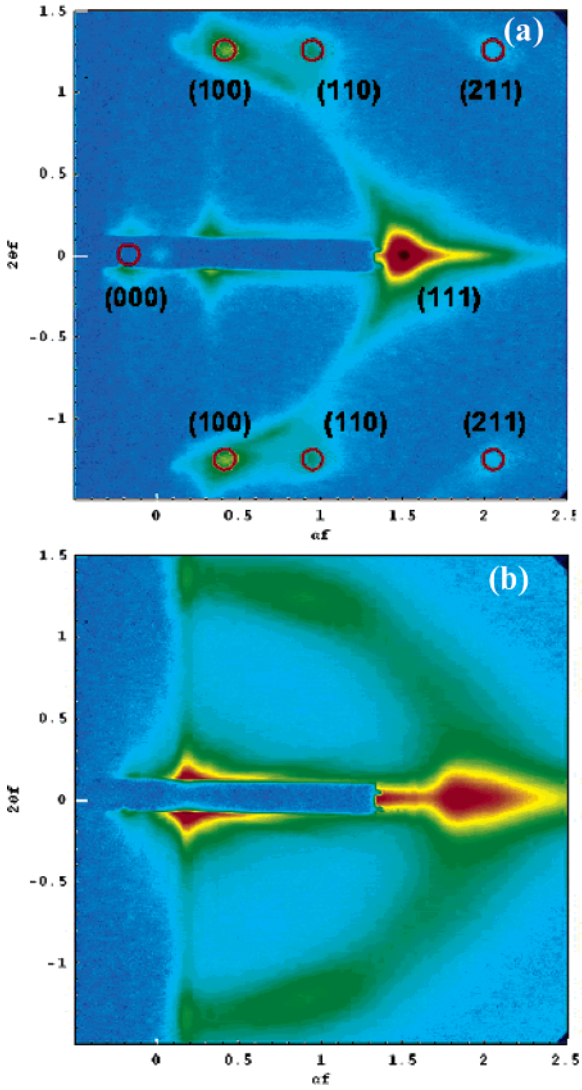

Figure 1. GISAXS patterns of as-synthesized (a) and calcined (b) films. Simulated diffraction spot pattern for a *R*-3*m* phase oriented with (111) planes parallel to the substrate is shown for the as-synthesized sample.

or narrow windows. Recently, Boissiere et al.,[7] by using environmental ellipsometric porosimetry, have shown that *Pm*3*n* and *Im*3*m* cubic structures have high pore accessibility from the air−substrate interface for molecules such as H_2O. The presence of unique *R*-3*m* mesostructure in our film was confirmed from GISAXS analysis for the as-synthesized and calcined samples as shown in Figure 1(a) and (b), respectively. The as-synthesized film shows a scattering pattern indicative of a film that is oriented relative to the plane of the substrate while sampling many rotational orientations relative to a vector perpendicular to the substrate.[5,6] A simulated diffraction spot pattern from a distorted cubic phase with its (111) plane oriented parallel to the substrate is overlaid on the data using NANO-CELL.[5] This simulated spot pattern explains the main features of the pattern. In addition, the slight arcing observed in the (111) diffraction spot is due to a small spread in orientation of the (111) plane relative to the substrate. There is additional intensity at $2\theta_f = 1.1°$ and $\theta_f = 0.8°$ that is not explained by this simulation which likely results from another orientation, (110) planes parallel to the substrate. The existence of multiple orientations within plane of a mesoporous silica films has already been demonstrated by Klotz et al. using TEM and GISAXS studies.[8] The GISAXS pattern from the calcined film shows features similar to the as-synthesized film. However, in

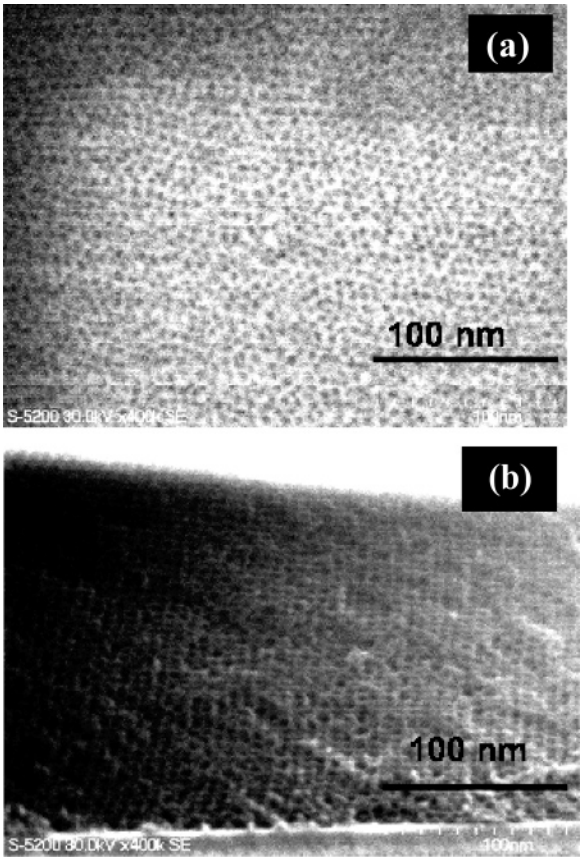

Figure 2. The top-view (a) and the cross-sectional (b) FE-SEM images, respectively, of the as-coated mesoporous silica film.

the calcined film there is stronger scattering along a ring, indicating a decrease in orientational order in the film. Further, the critical angle for X-ray scattering from the film is observed to decrease from around 0.25° to 0.17° upon calcination, indicating the removal of the surfactant and hence the reduction of the average electron density of the film. Eggiman et al.[9] have recently reported the fabrication of mesoporous silica films with *R*-3*m* mesostructure using Pluronic P123, a triblock copolymer, as a structure-directing agent. The orientation of the mesostructure in the bulk of their film was confirmed from comprehensive GISAXS analysis of the film. Furthermore, the effect of humidity and composition of silica−surfactant sol on the *R*-3*m* mesostructure was also studied by the same group.[10] Although topologically our film is identical to the one reported by Eggiman et al.,[9] notice that our film is fabricated using CTAB in the presence of TIPB. To the best of our knowledge, there is no literature on the existence of corresponding *R*-3*m* phase in the binary phase diagram of CTAB in water. In addition, the pore diameter of mesostructures synthesized using CTAB are typically in the range of 3−4 nm, in contrast to those synthesized using triblock copolymers that yield much larger mesostructures. The on-substrate FE-SEM images of the top and cross-sectional views of the as-coated film are shown in Figure 2(a) and (b), respectively, while the corresponding on-substrate TEM images of the calcined film are shown in Figure 3(a) and (b), respectively. These images reveal the highly porous and well-ordered *R*-3*m* structure in the film. The mesopores at the surface−air interface are clearly evidenced from these images. The N_2 adsorption/desorption plot and the BJH pore size distribution (adsorption branch) shown in Figure 4(a-i) and (b-i), respectively, further confirm the mesoporous structure of the film. The BET surface area of the film was 1000 m^2/g. The pore diameter and pore volume estimated by the BJH method

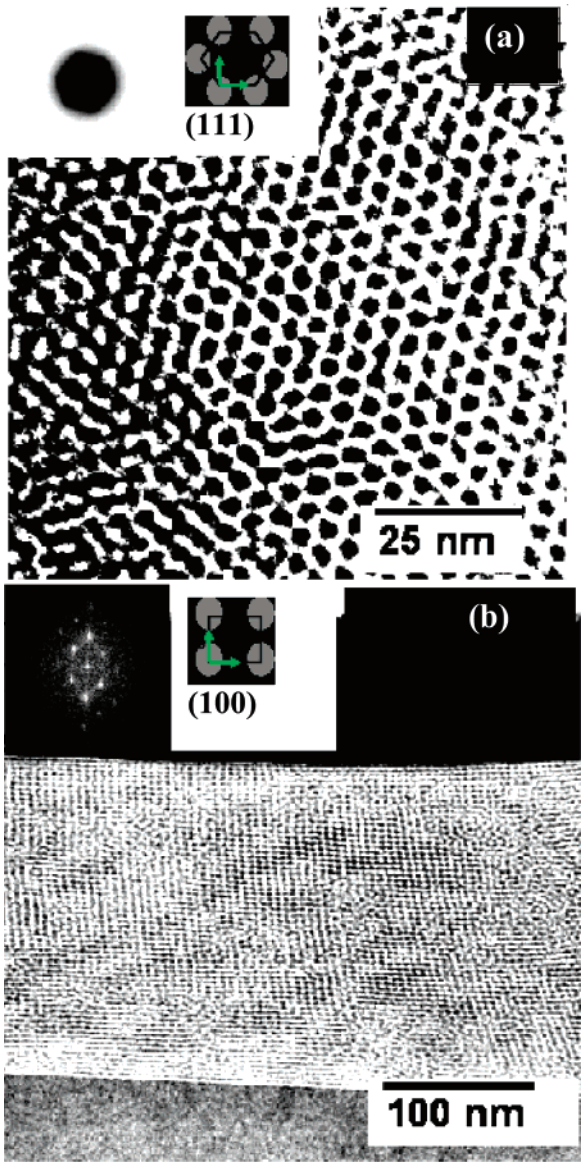

Figure 3. The top-view (a) and cross-sectional (b) TEM images of the as-coated film along the (111) and (100) planes respectively (inset are the electron diffraction patterns).

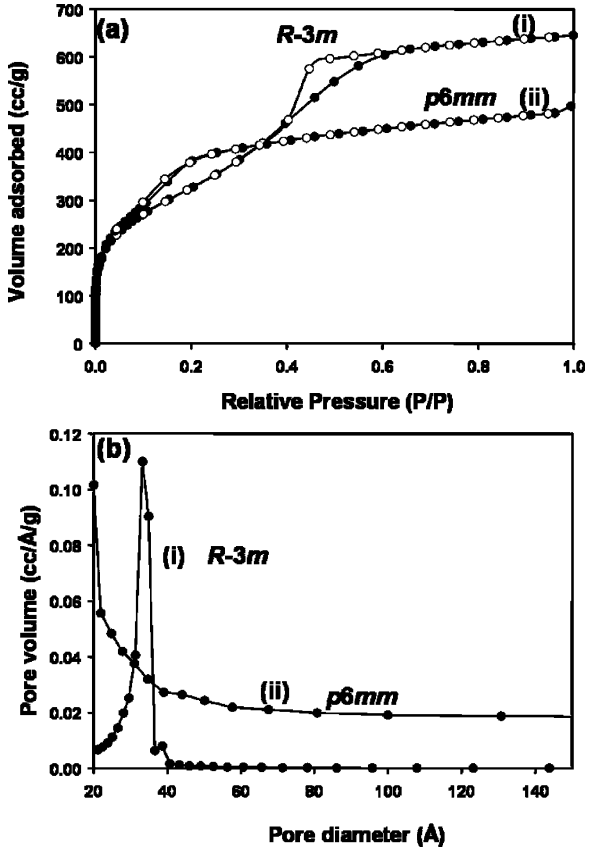

Figure 4. (a) Nitrogen sorption isotherms of the calcined mesoporous silica films peeled from the substrate (i) orthorhombic *R*-3*m* film (ii) hexagonal *p6mm* prepared from the same sol but at [TIPB] = 0. (b) Pore size distribution calculated by the Barrett Joyner Halenda (BJH) method for the two films.

were 3.4 nm and 1.0 cm^3/g, respectively. In contrast, the *p*6*mm* hexagonal film (Figure S.1, Supporting Information) synthesized from the same sol at [TIPB] = 0, shows much lower N_2 adsorption capacity and smaller pore diameter as shown in Figures 4(a-ii) and (b-ii), respectively. The BET surface area of the hexagonal film was 900 m^2/g, while the pore diameter and pore volume were 2.0 nm and 0.5 cm^3/g, respectively. The above results clearly demonstrate the presence of 3D open framework mesostructure of high porosity providing accessibility to molecules. In our work, the addition of TIPB to the silica/CTAB sol during the sol preparation was aimed to alter the micelle structure of the silica−surfactant composite in the liquid state. Previously it has been demonstrated by Luechinger et al.[11] that by adding a suitable hydrophobic additive to the SiO_2/surfactant gel, the geometry of surfactant micelle in liquid state can be changed due to the preferential location of hydrophobic additive in the micelle structure for the synthesis of mesoporous silica powders under alkaline conditions. Ryoo and co-workers have also demonstrated the exceptional control of the phase behavior of highly ordered large pore mesostructured silica powders (with the choice of *Fm*3*m*, Im3*m* or *p*6*mm* symmetry) using a triblock copolymer F-127 with butanol as an additive.[12] In our case, the TIPB molecules in the sol induce the formation of globular micelles due to their size-specific location in the SiO_2/CTAB micelle.[11,13] The transition from cylindrical micelle to spheroid that yields the 3D open mesostructure is driven by the requirement to cover an increased volume of TIPB with CTAB. TIPB swells out the hydrocarbon chains of the surfactant until saturation, and then pure TIPB core is formed at the center of the micelle. To cover the TIPB molecules with CTAB the micelle becomes more spherical, inducing the formation of 3D open mesostructure. We propose the formation of *R*-3*m* mesostructure through the distortion of intermediate 3D cubic, plausibly *Im*3*m*, mesophase formed during the film processing. Mesophase transformations upon drying/calcination in the films fabricated by evaporation-induced self-assembly (EISA) process are well-known.[10,14−19] Sanchez and co-workers[18] have also reported that, by adjusting processing conditions, a flexible metastable mesophase could be formed in films processed from SiO_2/CTAB sol at room temperature. It is also realized that film fabricated on solid substrates by EISA approach usually experiences a compression perpendicular to the film substrate due to possibly rapid formation of the film or stress induced during calcination. The manner in which the compression occurs has a strong influence on the pore topology of the film.[15,19] The formation of *Im*3*m* as an intermediate mesophase to *R*-3*m* is confirmed from the fact that the monolith obtained by slow drying of the coating sol in a Petri dish at room temperature showed *Im*3*m* cubic mesostructure (Figure S.2, Supporting Information). In this case, *Im*3*m* mesophase in the solid was stabilized at room temperature as it was not formed rapidly and

further unidirectional mesophase compression due to substrate was minimal or absent.

We have found that the addition of a hydrophobic additive TIPB is crucial for the formation of 3D mesostructure. Furthermore, the addition of TIPB did not produce precipitation or turbidity in the coating sol. Continuous and crack-free films could be, thus, easily fabricated by coating of the sol on various substrates. The study of pore accessibility of the film for solution phase species, particularly for electrodeposition of metals and semiconductor oxides, will be reported in due course.

Acknowledgment. The authors wish to acknowledge the financial support from Japan Science and Technology Corporation (JST). We also wish to acknowledge the use of the NSF funded facility for in-situ X-ray scattering from nanomaterials and catalysts (MRI program award 0321118-CTS) and the use of the Advanced Photon Source supported by the U.S. Department of Energy, Office of Science, Office of Basic Energy Sciences, under Contract No. W-31-109-ENG-38. We thank Prof. T. Tatsumi, Tokyo Institute of Technology, for the FE-SEM facility and Mr. H. Tsunakawa and Dr. K. Ibe, The University of Tokyo, for their technical assistance for TEM measurements.

Supporting Information Available: TEM images of *p*6*mm* hexagonal film and *Im*3*m* cubic mesostructure, respectively. This material is available free of charge via the Internet at http://pubs.acs.org.

References and Notes

(1) (a) Yanagisawa, T.; Shimizu, T.; Kuroda, K.; Kato, C. *Bull. Chem. Soc. Jpn.* **1990**, *63*(4), 988−992. (b) Kresge, C. T.; Leonowicz, M. E.; Roth, W. J.; Vartuli, J. C.; Beck, J. S. *Nature* **1992**, *6397*, 710−712. (c) Ogawa, M. *J. Am. Chem. Soc.* **1994**, *116*, 7941−7942.

(2) Lu, Y.; Ganguli, R.; Drewien, C. A.; Anderson, M. T.; Brinker, J. C.; Gong, W.; Guo Y.; Soyez, H.; Dunn, B.; Huang, M. H.; Zink, J. I *Nature* **1997**, *389*, 364−368.

(3) Uvray, X.; Petipas, C.; Anthore, R.; Rico, I.; Lattes, A. *J. Phys. Chem* **1989**, *93*(21), 7458−7464.

(4) Besson, S.; Ricolleau, C.; Gacoin, T.; Jacquiod, C.; and Boilot, J. P. *J. Phys. Chem. B* **2000**, *104*, 12095−12097.

(5) Tate, M. P.; Urade, V. N.; Kowalski, J. D.; Wei, T. C.; Hamilton, B. D.; Eggiman, B. W.; Hillhouse, H. W., *J. Phys. Chem.*, in press.

(6) Vineyard, G. *Phys. Rev. B* **1982**, *26*, 4146−4159.

(7) Boissiere, C.; Grosso, D.; Lepoutre, S.; Nicole, L.; Bruneau, A. B.; Sanchez, C. *Langmuir* **2005**, *21*(26), 12362−12371.

(8) Klotz, M.; Albouy, P. A.; Ayral, A.; Menager, C.; Grosso, D.; Van der Lee, A.; Cabuil, V.; Babonneau, F.; Guizard, C. *Chem. Mater.* **2000**, *12*, 1721−1728.

(9) Eggiman, B. W.; Tate, M. P.; Hillhouse, H. W. *Chem. Mater.* **2006**, *18*(3), 723−730.

(10) Tate, M. P.; Eggiman, B. W.; Kowalski, J. D.; Hillhouse, H. W. *Langmuir* **2005**, *21*, 10112−10118.

(11) Luechinger, M.; Pirngruber, G. D.; Lindlar, B.; Laggner, P.; Prins, P. *Microporous Mesoporous Mater.* **2005**, *79*, 41−52.

(12) Kleitz, F.; Solovyov, L. A.; Anilkumar, G. M.; Choi, S. H.; Ryoo, R. *Chem. Commun.* **2004**, 1536−1537.

(13) Lettow, J. S.; Han, Y. J.; Schmidt-Winkel, P.; Yang, P.; Zhao, D.; Stucky, G. D.; Ying, J. Y. *Langmuir* **2000**, *16*, 8291−8295.

(14) Ogura, M.; Miyoshi, H.; Naik, S. P.; Okubo, T. *J. Am. Chem. Soc.* **2004**, *126*, 10937−10945.

(15) Naik, S. P.; Ogura, M.; Sasakura, H.; Yamaguchi, Y.; Sasaki Y.; Okubo, T. *Thin Solid Films* **2006**, *495*, 11−17.

(16) Grosso, D.; Cagnol, F.; Soler-Illia, G.; Crepaldi, E. L.; Amenitsch, H.; Brunet-Bruneau, A.; Bourgois, A.; Sanchez, C. *Adv. Funct. Mater.* **2004**, *14*(4), 309−321.

(17) Soler-Illia, G.; Crepaldi, E. L.; Grosso, D.; Durand, D.; Sanchez, C. *Chem. Commun.* **2002**, 2298.

(18) Cagnol, F.; Grosso, D.; Soler-Illia, G.; Crepaldi, E. L.; Babonneau, F.; Amenitsch, H.; Sanchez, C. *J. Mater. Chem.* **2003**, *13*, 61−66.

(19) Crepaldi, E. L.; Soler-Illia, G.; Grosso, D.; Cagnol, F.; Ribot, F.; Sanchez, C. *J. Am. Chem. Soc.* **2005**, *125*, 9770−9786.